Molecular Crystals and Liquid Crystals
Publication details, including instructions for authors and subscription information:
http://www.tandfonline.com/loi/gmcl16

Charge-Transfer Excitons in Organic Solids

M. R. Philpott [a] & A. Brillante [a b]

[a] I.B.M. Research Laboratory, San José, California, 95193, U.S.A.

[b] IBM World Trade Postdoctoral Fellow 1977-1978. Laboratorio Spettroscopia Molecolare CNR, Via Castagnoli, Bologna, 40126, Italy

Version of record first published: 21 Mar 2007.

To cite this article: M. R. Philpott & A. Brillante (1979): Charge-Transfer Excitons in Organic Solids, Molecular Crystals and Liquid Crystals, 50:1, 163-174

To link to this article: http://dx.doi.org/10.1080/15421407908084423

Mol. Cryst. Liq. Cryst., 1979, Vol. 50, pp. 163–174

Printed in Holland

Charge-Transfer Excitons in Organic Solids

M. R. PHILPOTT and A. BRILLANTE†

I.B.M. Research Laboratory, San José, California 95193, U.S.A.

(*Received July 1, 1978*)

The polarized reflection spectra of single crystals of three weak charge transfer complexes have been measured at 2 K. The Kramers–Kronig transformation was used to calculate the complex frequency dependent dielectric functions from the reflection data. The oscillator strengths and the positions of the charge transfer exciton levels have been determined.

1 INTRODUCTION

The photo-induced separation of electric charges involving the transfer of an electron from one molecule to another, and the reverse phenomenon of electron-hole recombination with light emission, are processes that have long defied detailed quantitative experimental study in organic materials. In single component solids this has been due in part to the weakness and width of transitions to ionic states and also because of stronger overlying Frenkel exciton transitions.[1] Many of these difficulties are not present in multicomponent systems consisting of donor and acceptor molecules in fixed stoichiometry. For example in crystals of the weak charge-transfer complex pyrene-tetracyanoethylene, and many crystalline complexes like it, there are transitions to charge transfer states lying below the Frenkel exciton states of the donor and the acceptor molecules.[2] The charge transfer transitions are in all appearances analogous to singlet charge transfer transitions of complexes in solution.[3] In general these crystal transitions are broad and featureless, being devoid of fine structure that could be assigned to lattice phonons. At most the low temperature spectra consist of a series of broad bands several hundred cm^{-1} wide and 500 to 1500 cm^{-1} apart. These bands are thought to be due

† IBM World Trade Postdoctoral Fellow 1977–1978. Permanent address: Laboratorio Spettroscopia Molecolare CNR, Via Castagnoli, Bologna 40126, Italy.

to intramolecular vibrations excited by the electron transfer, that are broadened into envelopes by an unresolved series of multi-phonon transitions, that are also excited by the electron transfer process.

There is at present only one exception to the general rule that the transitions are broad and featureless. It has been shown that the visible fluorescence and transmission spectrum of the first singlet charge-transfer (CT) transition of the equimolecular complex anthracene-pyromellitic dianhydride (A-PMDA) has some sharp lines superimposed on the broad vibronic bands.[4-7] In the previously reported work on reflection and absorption the data were not corrected for lamp intensity distribution and reflectivity losses, respectively. Both of these effects distort the spectral contours sufficiently to impede the quantitative study of the reflectivity and absorption spectra.[8] The reflection spectra observed in these experiments show a prominent zero-phonon line, with a reflectivity up to 37% and a width of less than 5 cm^{-1}, as well as detailed phonon structure associated with the accompanying vibronic bands.

This paper describes some of the results of a program designed to provide detailed basic information about singlet charge transfer transitions in organic solids.[9] A detailed quantitative study of energy levels, like widths and intensity distributions in A-PMDA spectra should in principle provide insight into how the electron transfer process depends on nuclear coordinates of the donor and acceptor, and the vibrational state of the lattice. A study of CT transitions in other materials, while providing much less information, is nevertheless important as an indicator of those features of the A-PMDA results that have a general validity and are not specific to one particular solid.

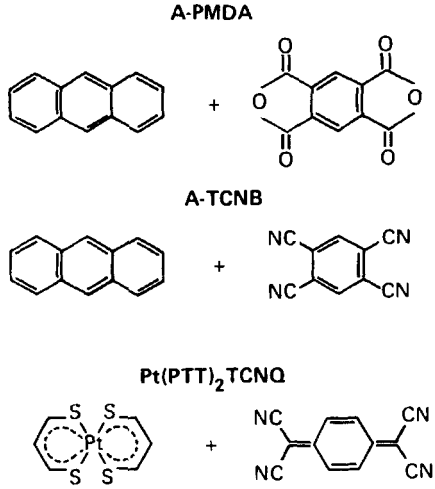

FIGURE 1 Structural formulas for the components of three weak charge transfer complexes.

The compounds chosen for this program have structural and chemical similarities. They are all quasi-one dimensional mixed stack crystalline organic complexes with a 1:1 stoichiometry. All the crystals were rather thick and because of this and the relatively high oscillator strength of the CT transition it was necessary to use reflection spectroscopy to measure the crystal spectra. The dielectric function was obtained by a Kramers–Kronig transformation of the reflectivity data.[10]

The compounds used in this program were: anthracene-pyromellitic dianhydride(A-PMDA); anthracene-tetracyanobenzene(A-TCNB); bis(propene-3-thione-1-thiolato) platinum (II)-7,7,8,8 tetracyanoquinodimethane (Pt $(PTT)_2$-TCNQ; pyrene-pyromellitic dianhydride (Py-PMDA); anthracene-tetracyanoquinodimethane (A-TCNQ); and phenanthrene-pyromellitic dianhydride (Ph-PMDA). The visible reflection spectra of these last three compounds were extremely weak and will not be described in any detail in this paper. In Figure 1 the structural formulas of the complexes A-PMDA, A-TCNB and $Pt(PTT)_2$-TCNQ are displayed.

2 NATURE OF CT EXCITONS

Charge-transfer excitons in mixed stacks have peculiar properties that make them very different to excitons in molecular crystals like naphthalene and anthracene.[6] The CT exciton is very polar and corresponds to an almost complete transfer of an electron from the highest filled donor orbital to the lowest unfilled acceptor orbital. This polar character has been verified experimentally in the case of A-PMDA by measuring the Stark shift of the CT transition when an electric field is applied parallel to the crystal stack axis.[5,6] With the electron and hole on separate molecules, strong coupling to the lattice is expected and manifestations of this interaction are the broad and relatively structureless absorption spectra due to the involvement of numerous lattice phonons. Another consequence of strong exciton-lattice coupling is the relaxation of the nuclei towards a new equilibrium position, and this leads at low temperatures to a self-trapping of the CT exciton. In the collapsed or self-trapped state the molecules are envisaged as having moved closer or reoriented in a way which lowers the energy of the excited state. Exciton motion is now hindered and may not occur by the usual direct transfer mechanism of Frenkel excitons in one component crystals, but by a polarity flipping process.[6]

In a one-dimensional mixed stack a donor molecule may lose its electron to the acceptors on either side. Likewise an acceptor molecule may receive an electron from the donor on either side. Some of the matrix elements describing transfer of the CT exciton along the chain are shown schematically

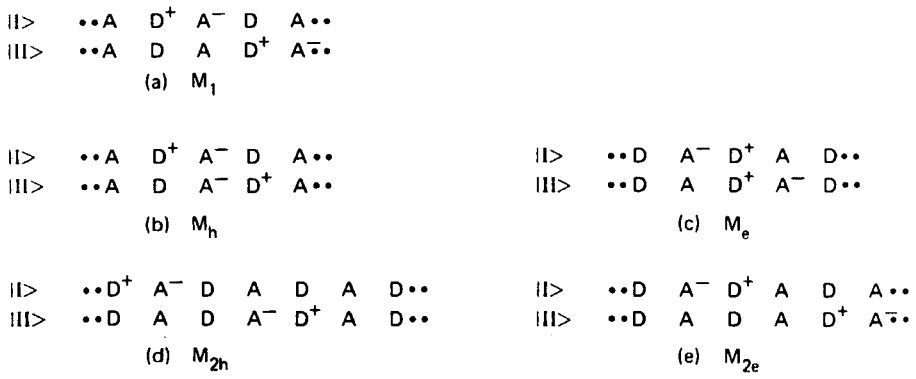

FIGURE 2 Schematic representation of various CT exciton transfer matrix elements: (a) exciton transfer without polarity flip, (b) hole transfer with polarity flip, (c) electron transfer with polarity flip, (d) and (e) exciton transfer with polarity flip. Kets $|\mathrm{I}\rangle$ and $|\mathrm{II}\rangle$ symbolize the initial and final stages, respectively.

in Figure 2. As a consequence of the CT exciton's polarity for a given k vector there are two exciton states. In a crystal with a center of symmetry the CT exciton states at $k = 0$ will have parity and only transitions to the odd parity state will be allowed from the ground state. However in the presence of an electric field applied parallel to the stack axis this symmetry is broken and the odd and even parity states are mixed together with the result that both are observed.

3 EXPERIMENT AND ANALYSIS

Crystals of A-PMDA, A-TCNB and $Pt(PTT)_2$-TCNQ were grown from solution using carefully purified materials. Details for A-PMDA are available elsewhere.[4,5] The samples selected for reflection spectroscopy generally had large faces, some as large as 5 × 5 mm.

The spectra were taken with the light at near normal angles of incidence, with the crystals immersed in superfluid liquid He at a temperature of approximately 2 K. The incident light was polarized parallel or perpendicular to the stack axis. A schematic diagram of the spectrometer and the detection system is shown in Figure 3. Absolute reflectivities were obtained by replacing the sample with a mirror of known reflectivity.

Peaks in the reflection spectrum of a solid do not occur at the same energy as peaks in the true absoption spectrum. Transverse exciton transitions correspond to maxima in the imaginary part of the dielectric function

$$\varepsilon(\omega) = \varepsilon_1(\omega) + i\varepsilon_2(\omega). \tag{1}$$

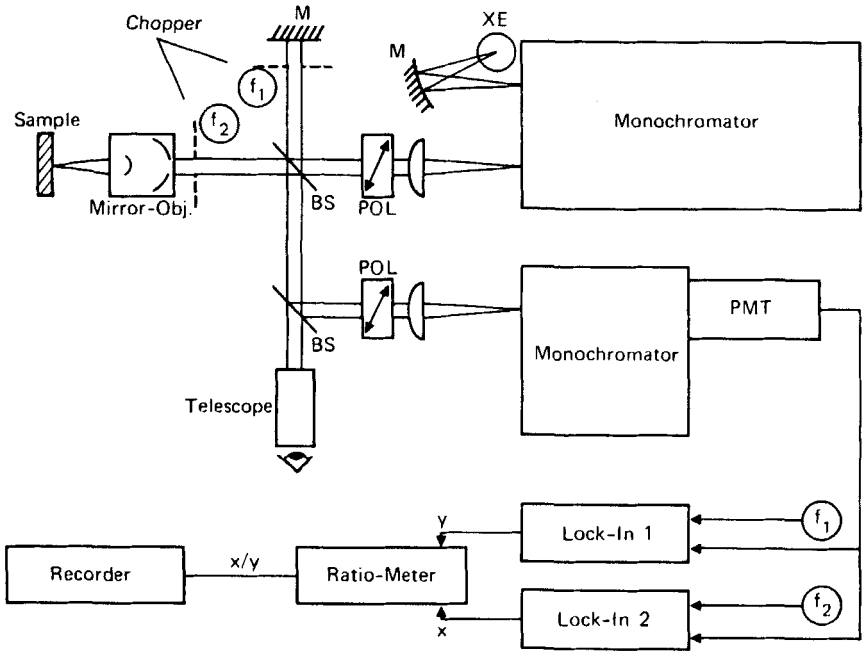

FIGURE 3 Schematic diagram of the reflection spectrometer.

Given the entire reflection spectrum function $R(\omega)$ where $1 \geq R(\omega) \geq 0$, the complex dielectric function $\varepsilon(\omega)$ can be obtained by means of the Kramers–Kronig transformation.[10] The key formulas are

$$\varepsilon(\omega) = \left\{\frac{1 + [R(\omega)]^{1/2} e^{-i\theta(\omega)}}{1 - [R(\omega)]^{1/2} e^{-i\theta(\omega)}}\right\}^2 \tag{2}$$

where the phase shift angle is defined by

$$\theta(\omega) = -\frac{\omega}{\pi} \int_0^\infty \frac{\ln R(\omega')}{(\omega')^2 - \omega^2} \, d\omega'. \tag{3}$$

Methods for evaluating the integral in Eq. (3) when only a limited frequency range has been measured are well documented.[10]

Once the dielectric function $\varepsilon(\omega)$ has been calculated the energies of transverse exciton transitions can be determined from the positions of the maxima in the $\varepsilon_2(\omega)$ spectrum. Other useful parameters are the stop-band width and the crystal oscillator strength. The width of a polariton stop-band is conveniently defined by $\Delta\omega = \omega_L - \omega_T$ where ω_L is the longitudinal exciton peak in the function $-Im\varepsilon^{-1}(\omega)$. The oscillator strength of any region of the

spectrum is defined by

$$f_{ab} = \left(\frac{mv_c}{4\pi^2 e^2 \sigma}\right) \int_a^b \omega \varepsilon_2(\omega)\, \mathrm{d}\omega$$

where v_c is the volume of a unit cell and σ is the number of DA complexes in a unit cell.

4 RESULTS AND DISCUSSION

The main results of the reflection measurements will be discussed in turn for each of the three complexes.

4.1 A-PMDA

The crystals of A-PMDA are triclinic, probable space group $P\bar{1}$, with one molecule of each component per unit cell.[11] The crystals are generally elongated along the stack axis, which is the crystallographic c axis, with donor and acceptor molecules alternating in a quasi-one dimensional chain in which the intermolecular separation is 3.23 Å.

The reflection spectrum for light polarized parallel to the stack axis, is shown in Figure 4. In the region of the CT transition, the spectrum consists of a series of six or possibly seven broad bands, each approximately 500 cm^{-1} wide, which are presumed to be of intramolecular origin, i.e., they arise from the excitation of the internal modes of the anthracene and PMDA molecules.

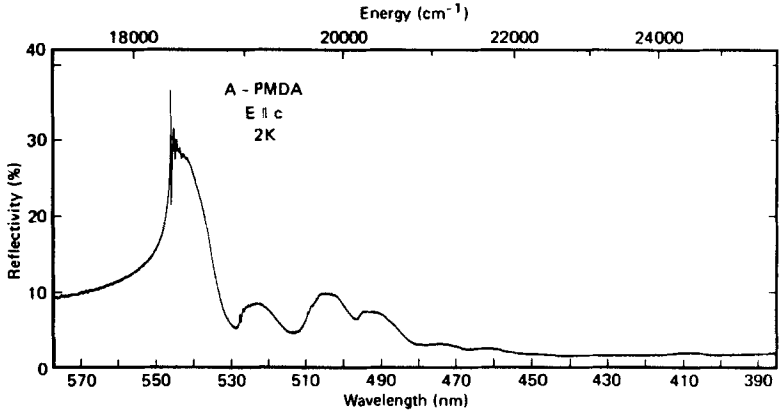

FIGURE 4 Reflection spectrum of an A-PMDA single crystal taken at near normal incidence and at a temperature of 2 K for light polarized with electric vector parallel to the stack axis.

These broad bands are referred to as the 0–0, 0–1, 0–2, . . . , etc. bands. At much higher energy, a weak broad band near 410 nm, probably due to a $\pi\pi^*$ system of anthracene, is observed. It is weak because of a poor projection of the transition dipole moment onto the stack axis and because the oscillator strength per unit cell is approximately one half of that of the anthracene crystal.

Whereas the broad bands have their origin in the intramolecular vibrations the fine structure impressed on the 0–0, 0–1 and 0–2 bands is almost certainly of intermolecular nature originating from the lattice modes excited by the transfer of the electron from the donor to the acceptor molecule. The fine structure is most prominent in the region of the origin of the 0–0 band. Figure 5 shows a detail of this band and the corresponding $\varepsilon_1(\omega)$ and $\varepsilon_2(\omega)$ spectra derived by the Kramers–Kronig transformation. The zero-phonon line is by

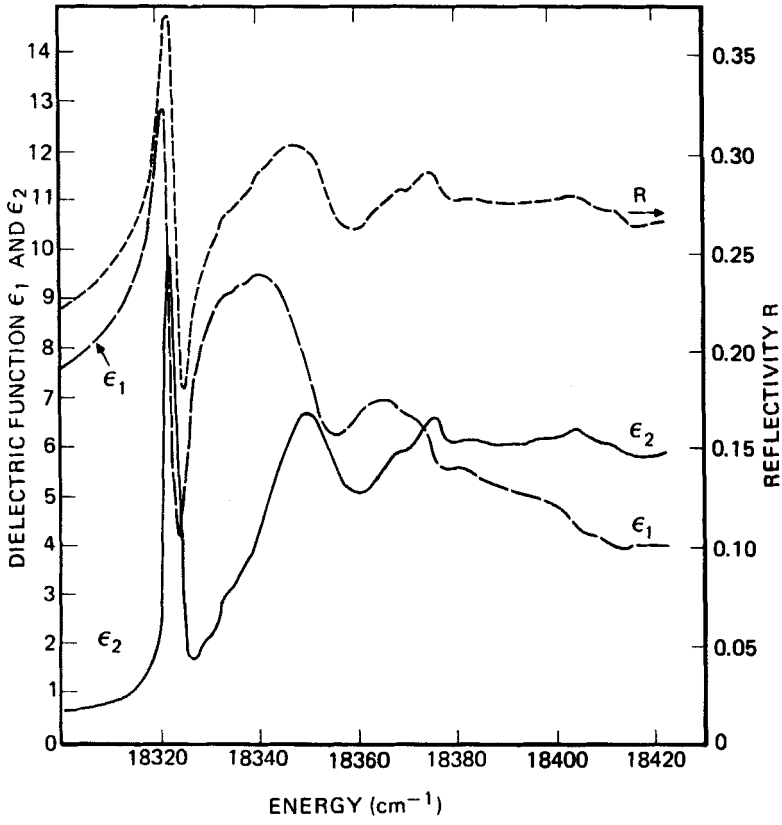

FIGURE 5 Detail of the reflection, $\varepsilon_1(\omega)$ and $\varepsilon_2(\omega)$ spectra of A-PMDA in the region of the zero-phonon line of the 0–0 band.

TABLE I

Summary for the 0-0 Region of A-PMDA

Band	$\hbar\omega_T$ (cm^{-1})	Difference $\hbar\omega_T - \hbar\omega_{0\text{-}0_0}$	Comments
1	18,321	0	zero phonon line $0\text{-}0_0$
2	18,334	~13	weak shoulder
3	18,347	26	weak shoulder
4	18,350	29	max
5	18,363	42	shoulder
6	18,369	47	shoulder
7	18,376	55	max; $2 \times \nu_4$
8	18,383	62	max
9	18,398	~77	weak shoulder
10	18,404	83	max; $3 \times \nu_4$
11	18,409	88	shoulder
12	18,432	111	max; $4 \times \nu_4$
13	18,463	142	max; $5 \times \nu_4$

far the sharpest and most intense feature in the reflection spectrum and relative to this line there are phonon peaks at 27, 47, 53, 62, 83, 111, 142 cm^{-1} in the reflection spectrum. In the $\varepsilon_2(\omega)$ spectrum the corresponding phonon peaks are at 29, 47, 55, 62, 83, 111 and 142 cm^{-1}. These results are summarized in Table I. The peaks at 47 and 62 may be related to the known low temperature Raman modes of the crystal.[7] However, the lowest peak at 29 cm^{-1} and its possible multiples at 55, 83, 111 and 142 cm^{-1} have no known counterparts in either the normal or pre-resonance Raman spectrum.[12] Phonons of similar low frequency have also been detected in the 0–1 and 0–2 regions.

The existence of low frequency lattice modes in organic molecular DA complexes has been previously reported only for *phosphorescence* emission spectra of pyrene-PMDA in a naphthalene-PMDA host crystal by Beckmann and Small.[13] In this system, there is a zero-phonon line and multi-phonon progression that looks very similar to that seen in *absorption* in A-PMDA. However, in A-PMDA this is the first time that they have been clearly identified in a *singlet* CT absorption spectrum and for a "neat" crystal.

The qualitative agreement, with the exception of the 29 cm^{-1} phonon and its multiples, of the observed low frequency structure with the corresponding ground state lattice modes observed in the Raman spectrum, provides a first phenomenological interpretation of the observed spectral contours. As a consequence, the main question at the present stage lies in the interpretation of the 29 cm^{-1} phonon. According to the view that phonon sidebands represent state density distribution of lattice vibrations, the most likely interpretation at the moment is to assign this low frequency phonon to an A_g mode, possibly an acoustical mode, strongly coupled to the ionic

upper state. The physical basis of this strong coupling is under investigation. Alternative explanations may, of course, be advanced, such as: (i) low frequency local phonon associated with a collapsed excited state in which there is no longer any translational symmetry and for which the phonon has no ground state counterpart; (ii) an IR phonon that has as its origin the totally symmetric g electronic state located 10 cm^{-1} above the zero-phonon line of the first CT transition, in which case the frequency of the phonon with u symmetry will be 19 cm^{-1}; (iii) a double quantum of a u fundamental phonon. Also under consideration is a simple theoretical model in which the D and A molecules have equal mass. In this model, which has applications to one component crystals, the exciton-phonon interaction induces a doubling of the "phonon" unit cell with the result that the longitudinal acoustical branch is folded back, thereby creating an optical $k = 0$ phonon of low frequency.

4.2 A-TCNB

Crystals of A-TCNB are monoclinic at room temperature with two donors and two acceptors per unit cell.[14] The stack axis of both chains is parallel to the crystallographic c axis. There is evidence that the crystal undergoes a phase transition at 205°K that decreases the crystal symmetry.[15] The structure of the low temperature phase is not known at present.

In Figure 6 we show the reflection spectrum of A-TCNB taken with light polarized parallel and perpendicular to the stack axis. There are two main bands at 510 and 474 nm and a third weak band at 458 nm. These bands will be referred to as the 0–0, 0–1 and 0–2 bands, respectively. In the $\perp c$ spectrum there is a weak band at 390 nm that corresponds to the onset of the anthracene Frenkel exciton transitions. Note that although the reflectivity of the 0–0 region is comparable with the 0–0 region of A-PMDA, there is no fine structure due to lattice phonons.

The reflection spectrum of CT transition has been transformed to obtain the complex dielectric function. Table II summarizes the main results derived

TABLE II

Summary of the oscillator strength, transverse and longitudinal exciton energies in A-TCNB

Band	$\hbar\omega_T$ (cm^{-1})	$\hbar\omega_L$ (cm^{-1})	$\hbar\Delta\omega$ (cm^{-1})	Oscillator strength f
0–0	19,580	20,110	530	0.2
0–1	21,130	21,400	270	0.1
0–2	21,830	21,860	30	0.0

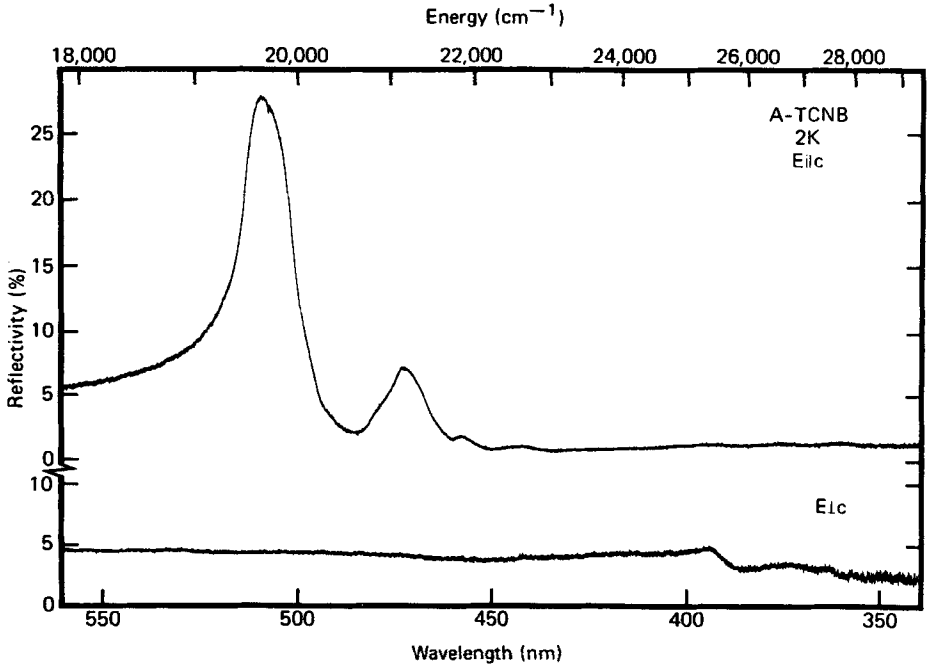

FIGURE 6 Reflection spectrum of an A-TCNB crystal taken at near normal angles of incidence at a temperature of 2 K for light polarized parallel and perpendicular to the stack axis (c).

from this calculation. The polariton stop-band for the 0–0 region is over 500 cm^{-1} wide, and the oscillator strength is also large. The total linear oscillator strength of the CT transition obtained from an integration from 17,300 cm^{-1} to 24,630 cm^{-1} is 0.3. This means that in A-TCNB the intrinsic strength of the CT transition is comparable to the first singlet transition of anthracene.

4.3 $Pt(PTT)_2$-TCNQ

The polarized reflection spectrum of $Pt(PTT)_2TCNQ$ is shown in Figure 7. There are three spectral regions, the first at 600 nm is due to the CT exciton, the second between 500 nm and 400 nm has components in both polarizations and is probably due to a Frenkel state of TCNQ°, the third at 350 nm is also polarized parallel and perpendicular to the stack axis and is assigned to a metal-ligand transition on the donor.

The reflectivity of the CT region is much lower than for either A-PMDA and A-TCNB and corresponds to a much smaller oscillator strength. The

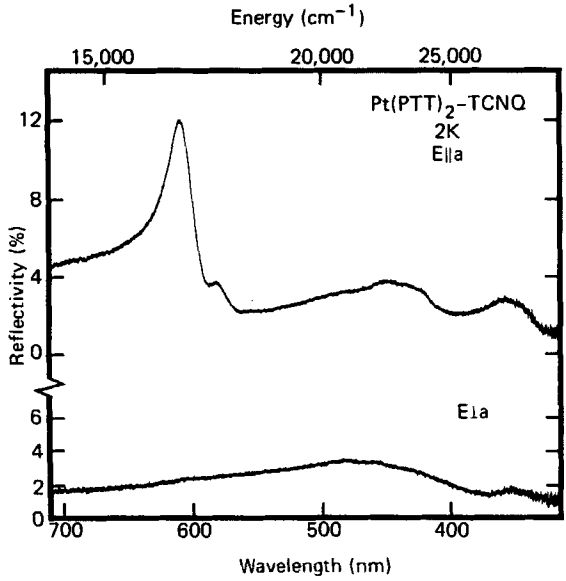

FIGURE 7 Polarized reflection spectrum of a $Pt(PTT)_2$-TCNQ crystal taken at near normal angles of incidence at a temperature of 2 K for light polarized parallel and perpendicular to the stack axis (a).

TABLE III

Summary of the oscillator strength, transverse exciton and longitudinal exciton energies for $Pt(PTT)_2$-TCNQ

Band	$\hbar\omega_T$ (cm^{-1})	$\hbar\omega_L$ (cm^{-1})	$\hbar\Delta\omega$ (cm^{-1})	Oscillator strength f
1 (0–0)	16,500	16,770	270	0.1
1 (0–1)	17,250	17,360	110	
2	23,080	—	—	0.1
3	28,740	—	—	0.1

CT transition consists of two broad structureless peaks separated by 750 cm^{-1}. Table III summarizes the data obtained by Kramers–Kronig transformation of the ∥ a reflection spectrum. Even though the reflectivity of the TCNQ° and the metal-ligand transitions are lower their oscillator strengths are high. The explanation of this lies in the greater breadth and higher energy of these transitions.

Acknowledgments

We wish to thank J. Duran for purifying and growing the A-PMDA and A-TCNB crystals, and U. Muller-Westerhof and J. Mayerle for providing the $Pt(PTT)_2$-TCNQ crystals.

References

1. See, for example, D. M. Hanson, *Crit. Rev. Solid State*, **3**, 243 (1973).
2. H. Kuroda, I. Ikemoto and H. Akamatu, *Bull. Chem. Soc. Japan*, **39**, 1842 (1966).
3. See, for example, R. Foster, "Organic Charge-Transfer Complexes," (Academic Press, New York, 1969).
4. D. Haarer and N. Karl, *Chem. Phys. Lett.*, **21**, 49 (1973).
5. D. Haarer, *Chem. Phys. Lett.*, **27**, 91 (1974); **31**, 192 (1975).
6. D. Haarer, M. R. Philpott and H. Morawitz, *J. Chem. Phys.*, **63**, 3238 (1975).
7. D. Haarer, *J. Chem. Phys.*, **67**, 4076 (1978).
8. A. Brillante, M. R. Philpott and D. Haarer, *Chem. Phys. Lett.*, **56**, 218 (1978).
9. A. Brillante and M. R. Philpott, unpublished observations.
10. F. Stern, *Solid State Physics*, **15**, 299 (1963).
11. J. C. H. Boeyens and F. H. Herbstein, *J. Phys. Chem.*, **69**, 2153 (1965).
12. R. W. Syme and R. Macfarlane, unpublished observations.
13. R. L. Beckman and G. J. Small, *Chem. Phys. Lett.*, **30**, 19 (1978).
14. H. Tsuchiya, F. Maruma and Y. Saito, *Acta Cryst.*, **B28**, 1935 (1972).
15. H. Möwald and E. Sackmann, *Solid State Comm.*, **15**, 445 (1974).
16. J. J. Mayerle, *Inorg. Chem.*, 16, 916 (1977).